COSMIC RAYS AND SOLAR PROTONS IN THE NEAR-EARTH ENVIRONMENT AND THEIR ENTRY INTO THE MAGNETOSPHERE

S. B. Gabriel

Department of Aeronautics and Astronautics, University of Southampton, England

ABSTRACT

Energetic solar particle events (SPE) and galactic cosmic rays (GCR) can have a significant effect on the design and operations of interplanetary and earth-orbiting spacecraft. They produce high energy protons and heavier ions, which can cause radiation degradation of electronic parts, sensor interference and single event effects. Although both environments are modulated by solar activity effects, GCR fluxes are always present while SPEs occur sporadically throughout the solar cycle. A description of the particle fluxes is presented in terms of their source, acceleration mechanisms, energy spectra and composition, directionality, transport through interplanetary space to the boundary of the earth's magnetosphere and finally through the magnetosphere to lower altitudes. The relevance of both sets of particle fluxes is discussed in the context of Space Weather. Emphasis is given to the underlying physical processes involved but current engineering models and their inadequacies are also discussed. The prospects for prediction are addressed in terms of our present state of knowledge, including the issues involved in separating causes from associations.

1. INTRODUCTION

The present consensus is that Fermi acceleration by supernova shock-wave remnants is responsible for the production of cosmic rays in our galaxy and that subsequently they propagate in the Galactic magnetic field. Within the heliosphere, galactic cosmic ray fluxes are modulated by the eleven year cycle of solar activity, with the minimum occurring at solar maximum. A simple explanation of this anti-correlation is given in terms of solar wind variations and the three key processes, essential for an understanding of cosmic ray propagation in the heliosphere, diffusion, convection and adiabatic deceleration, are briefly described.

SPEs occur at active sites on the sun, producing fluxes of high energy protons, heavy ions and electrons. The current view is that particle acceleration is caused by coronal mass ejection (CME) driven shocks in the corona and interplanetary medium. Propagation takes place along the interplanetary magnetic field and the dependence of the event intensity, at a particular spacecraft location, on the heliolongitude of the production site is discussed. The propagation and radial dependence of SPE fluxes are governed by the same processes involved in GCR transport. Unlike GCR fluxes, there is no clear dependence of SPE fluxes on solar cycle activity, although the larger events occur during a seven year period, centred on the maximum and extending 2 years prior to and 4 years after it.

The earth's magnetic field shields both SPE and GCR particles from penetrating to low altitudes; the basic physics of this process of geomagnetic shielding is explained , including the key concepts of magnetic rigidity and minimum cut - off energy, the energy below which an ion cannot reach a given point in the earth's dipolar field. Due to the interaction with the solar wind, the earth's dipole field is distorted, giving rise to a region known as the magnetosphere. Large geomagnetic storms, an important aspect of Space Weather, disturb the magnetosphere and lower the cut-off rigidity, posing potential radiation hazards for spacecraft in low altitude, low inclination orbits. Since these large geomagnetic disturbances are caused by fast CMEs, it is possible to have the simultaneous occurrence of a large SPE and a disturbed magnetosphere. Recent spacecraft measurements of SPE fluxes during periods of high geomagnetic activity, both outside and within the magnetosphere, are reviewed along with comparisons of theoretical and measured values of geomagnetic transmission.

2. COSMIC RAYS

2.1 Origins and Acceleration

There are two constituents of what are commonly called cosmic rays, galactic cosmic rays (GCR) and anomalous cosmic rays (ACR). The present consensus is that Fermi acceleration by supernova shock-wave remnants is responsible for the production of the GCR component (Ref. 1). Anomalous cosmic rays are thought to originate as neutral interstellar gas that drifts into the heliosphere, becomes singly-ionised near the sun and then is convected to the outer heliosphere where it is accelerated to higher energies (Ref. 2).

2.2 Propagation and Time Variations

Propagation and time variations are treated together because long term, solar cycle time variations at the earth are caused by propagation of the cosmic rays from outside of the heliosphere into it; the simple view is that the expanding solar wind exerts a pressure on the interstellar charged particles, modifying their entry into the heliosphere (Fig. 1 and Ref. 3). At solar maximum the solar wind pressure is higher producing lower cosmic ray fluxes while the reverse is true at solar maximum. The propagation is in fact much more complex being governed by the balance between the three main physical processes of diffusion, convection and adiabatic deceleration. The current view is that all of the essential physics is contained in the equation (Ref. 4) :

$$\frac{\partial n}{\partial t} = \nabla \cdot \kappa \cdot \nabla n - \nabla \cdot (Vn) - v_D \cdot \nabla n + \frac{1}{3} \nabla \cdot V \frac{\partial}{\partial T}(\alpha T n) \qquad (1)$$

n = differential number density per unit kinetic energy,T
κ = diffusion tensor
V = solar wind speed
v_D = effective drift speed in mean magnetic field
$\alpha(T) = (T + 2T_0)/(T + T_0)$ where T_0 = particle rest mass energy.

The first term on the RHS represents diffusion amongst irregularities in the solar wind magnetic field, with different values of κ perpendicular to and parallel to the magnetic field. The second describes convection with the solar wind speed, and the third, drift in the mean magnetic field. The last term is

the adiabatic deceleration one, and is similar to adiabatic cooling of an expanding gas.

The cosmic ray fluxes are modulated by solar activity, showing an 11 year period as illustrated in Figure 2 (Ref. 5), with the highest fluxes occurring at solar minimum and the lowest at solar maximum, i.e. an anti-correlation with solar activity. This modulation is energy or rigidity dependent with low to medium energies ($\lesssim$ 1GeV/nucleon) showing the most effect. In addition to these long term temporal changes, there are shorter term fluctuations, called Forbush decreases (Ref. 5), which are thought to be caused by large interplanetary shocks. One view is that solar activity decrease is caused by a series of these much shorter Forbush events. There is also a 22 year modulation induced by the reversal of the polarity of the sun's magnetic field every 22 years; this effect can be explained by the effective drift speed term (third term on RHS in equation 1), which will also change sign.

2.3 Energy Spectra and Composition

Typical spectra, during a solar minimum period from 1974 to 1978, for energies below about 1GeV/nucleon, are shown in Figure 3 (Ref. 6). The fluxes of several elements, especially, He, N, O and Ne are enhanced below about 50 MeV/nucleon and this is the anomalous component. Figure 4 (Ref. 7) shows the differential energy spectrum for three elements up to energies of 1000GeV/nucleon. At lower energies, of the order of 1GeV/nucleon, solar cycle modulation effects are illustrated, the upper envelope indicating the spectrum at solar minimum, the lower at solar maximum and the shaded region the range over one cycle. The hydrogen spectrum in this figure has been multiplied by 5, to prevent overlap with the upper envelope of the He spectrum. At high energies, >5 GeV/nucleon, the spectra approach the well known $E^{-2.7}$ form (Ref. 1) and all elements have approximately the same spectral shape, although there is an enhanced abundance of Fe at high energies and relative depletion of H at lower energies.

Figure 5 (Ref. 6) shows the composition of cosmic rays normalised to Si = 10^6. There is a >10 decades range in relative fluxes between hydrogen and the heaviest elements. The elemental composition is roughly in proportion to the solar system distribution but with some differences; there is an enhancement of "secondary nuclei" produced by fragmentation, e.g. Li, Be, and B, a relative depletion by ~5 of elements with high first ionisation potential (e.g. C, N, O, Ne, Ar) and an underabundance of H and He relative to the heavier elements.

3. SOLAR PROTONS

3.1 Origins and Acceleration

There are many sources of solar protons ranging in energies from around 1keV (solar wind) to greater than 500MeV. Only those particles with energies from about 1MeV and above, produced in what are called solar energetic particle events (SEPEs) or solar proton events (SPEs) are discussed herein. These events are sporadic in nature, occurring at any time throughout the solar cycle and exhibiting a wide range in duration (2–20 days) and fluxes (5 to 6 orders of magnitude). From 1963 to the present, solar proton fluxes have been observed using a series of closely related instruments on the spacecraft IMP 1, 2, 3, OGO 1, Imp 5, 6, 7 and 8 and more recently the GOES series (Ref. 8). Fluences (time integrated flux over event duration) can vary from just above the cosmic ray background to of the order of 10^{10} p/cm^2 at energies, E > 10 MeV as in the case of the October 1989 event. Event fluences $\gtrsim$ 1.5 x 10^9 p/cm^2 (E > 10 MeV) are very rare with there having been only about 14 since 1963. There were no events with > 10^{10} p/cm^2 at E > 10 MeV between the famous August 1972 event and the October 1989 one; the 1972 event and its associated geomagnetic storm caused widespread power outages in Canada and the USA.

The mechanism responsible for proton acceleration and the cause of SPEs are subjects which are widely discussed in the literature, with much controversy in particular over the role of flares (Refs. 9, 10). However, it appears that the generally accepted view is that particle acceleration, in the largest events, is caused by coronal mass ejection (CME) driven shocks in the corona and interplanetary space. There is growing evidence that there are two types of events, impulsive and gradual, whose characteristics are shown in Table 1.

	Impulsive	Gradual
Particles:	Electron-rich	Proton-rich
3He/4He	~1	~0.0005
Fe/O	~1	~0.1
H/He	~10	~100
QFe	~20	~14
Duration	Hours	Days
Longitude Cone	<30 deg	~18- deg
Radio Type	III, V (II)	II, IV
X-rays	Impulsive	Gradual
Coronagraph	-	CME (96%)
Solar Wind	-	IP Shock
Events/year	~1000	~10

Table 1. Properties of Impulsive and Gradual Events

(From Ref. 11).

In Gradual events the particles have elemental abundances and isotopic compositions characteristic of the corona and apparently arise from regions that have an electron temperature of 1-2MK. On the other hand, impulsive events show a marked enhancement of heavy ions, He^3/ He^4 ratios 2-4 orders of magnitude larger than in the solar atmosphere or solar wind; they are dominated by electrons and the composition suggests that the ions come from deep within the corona (T_e ~3-5MK). It would appear that the particles associated with these events are directly accelerated in solar flares.

3.2 Propagation

Figure 6 shows the propagation of solar energetic particles from their site of production on the sun to the earth (Ref. 12). Particles propagating to the earth along magnetic field lines in the solar wind will be anisotropic when they reach the earth but the majority will be scattered many times and therefore will be isotropic. The propagation time (between event and appearance of protons at the earth) is a strong function of the longitude of the solar event (Figure 7, Refs. 13,14). Protons can arrive from well-connected sites in tens of minutes; the most effective for E > 10 MeV protons is ~ 30^0 W but the distribution about this longitude is very wide. For particles in the GeV range, the most effective longitude is close to 60^0 W (Ref. 15).

3.3 Time Variations

There is no clear solar cycle dependency of solar proton event fluences, certainly in terms of event occurrences, with events taking place at any time throughout a cycle. Nevertheless, Feynman et al (Ref. 16) found that, by defining the year of sunspot maximum to 0.1 year, the annual integrated fluence could be divided into two periods, a high fluence active sun period of 7 years and a low fluence, quiet sun one of 4 years. The active period extends from 2 years before the year of solar maximum to 4 years after, as illustrated in Figure 8. For sunspot numbers greater than 50 there is no correlation of fluences with sunspot number; the sunspot number at the time of the great event of November 1960 was < 60 and < 90 when the August 1972 event occurred (Ref. 17).

On shorter time scales of the order of the duration of the event, the particle fluxes rise over a period of ½ -1 day with a slower decay of about a few days. These features are evident in Figure 9, which shows the fluxes for two major events and are quite characteristic of proton events in general. However, the second strong increase at the end of the first decay phase is only found in the largest of events and is due to a series of CMEs and shocks.

3.4 Energy Spectra

Solar proton events exhibit a wide range both in their fluence and peak flux spectra. Fluence spectra for three of the largest events ever measured are shown in Figure 10, along with fitted curves. For the August 1972 and November 1960 events, the spectra have the form of an exponential in energy, while the October 1989 event follows a power law in energy. The hardness of the spectrum and its form is a key factor in determining effects on electronic parts, with low to medium energies (4-10 MeV) being most important for solar cell degradation, for example, and the higher energies ($\gtrsim$ 100 MeV) for single event effects (SEEs).

4. GEOMAGNETIC SHIELDING

4.1 Introduction

When both cosmic rays and solar protons (and ions) reach the earth they are impeded from reaching certain locations due to their interaction with the earth's magnetic field. The extent to which their trajectories are influenced by the $\underline{v} \times \underline{B}$ force is determined by their rigidity, R or momentum divided by charge:

$$R = pc/q \qquad (2)$$

where p = momentum
c = speed of light
q = charge.

Whether a charged particle reaches a specific location on the earth's surface or in an orbit, is also dependent on the direction in which the particle is travelling and the magnetic latitude of the point. Because of the non-linearity of the equations of motion, they cannot be solved analytically. However, Störmer in his classic work on aurora about 50 years ago (Ref. 18) developed some useful analytic approximations for the minimum value of the cut-off rigidity, R_c, which are still used today. Because of its widespread use and utility, a very brief description of the major results of Störmer theory is given in the next section.

4.2 Störmer Theory

Störmer theory assumes that the earth's magnetic field is a simple dipole, ignoring the offset and tilt, shielding by the solid earth and any external (e.g. ring current) contributions. The equation often quoted for the minimum cut-off rigidity (Ref. 17) is

$$R_C = [C_S \cos^4\lambda]/\{r^2[\,1+ (1 - \sin\varepsilon\sin\zeta\cos^3\lambda)^{\frac{1}{2}}\,]^2\} \qquad (3)$$

where C_S is a constant related to earth's magnetic dipole moment and equal to 59.6 for a dipole moment of 8.06 10^{25} gauss cm^3 (appropriate for circa 1930s to 1950s) and 58 for a dipole moment of 7.84 10^{25} gauss cm^3 (based on the 1990 International Geomagnetic Reference Field (IGRF).

λ = magnetic latitude
ε = angle from zenith direction (where zenith direction is a radial from the dipole centre)
ζ = azimuthal angle measured clockwise from the direction to the north dipole axis and
r = radius normalised to the radius of the earth
(R_C is in GV).

A useful approximation for the lowest value, R_{CW}, which is from the magnetic West is

$$R_{CW} = [C_s\cos^4\lambda]/\{r^2[\,1+ (\,1+ \cos^3\lambda)^{1/2}]^2\} \qquad (4)$$

The variation of R_C with λ is shown in Figure 11 (Ref. 20) for ε = 60° and vertical, east and west directions and illustrates that high energy cosmic rays can reach latitudes of about 55° while a 50 MeV proton cannot penetrate below a magnetic latitude of about 70°. Figure 12 gives a geometric picture of the three separate regions predicted by Störmer theory, the forbidden cone about the magnetic east direction, the allowed or main cone around the magnetic west (Ref. 21) and the penumbra region where particle trajectories are chaotic (Ref. 19).

4.3 Depression of Cut-off Rigidity during High Geomagnetic Activity

As mentioned previously, Störmer theory assumes that the earth's magnetic field is a simple dipole and does not take into account any external current effects. During geomagnetically quiet periods, the cut-off rigidity given by Störmer theory (eqn. 2) is a fairly good estimate. But during periods of high activity i.e. a large geomagnetic storm, observations show that the cut-off rigidity is significantly lower than that predicted by Störmer theory i.e. particles with much lower energies/rigidities can reach a given location. Measurements from CRRES (Ref. 22) showed that during a large SPE in March 1991 26MeV protons reached L values of < 3 R_E; Störmer theory gives an access cut-off value for this energy of 7 R_E. This event was also responsible for the formation of a new trapped radiation belt between 2 and 3 R_E (Ref. 22), which appeared to be quite stable for the remainder of the CRRES mission. Little work has been done on the modelling of the lowering of the geomagnetic cut-off during high geomagnetic activity. Probably the most detailed, recent work is by Boberg et al (Ref. 23), in which various magnetic field models are used to calculate the orbit averaged geomagnetic transmission factors based on NOAA 10 and GOES 7 36-80 MeV proton fluxes during the large October 1989 SPE. By using trajectory tracing and the IGRF model for the earth's internal field coupled with a modified version of the

Tsyganenko model (Ref. 24) for the average fields from magnetosopheric currents, they obtained much closer agreement to the data than use of IGRF grid calculations (Fig. 13), quiet time parameterisation (Ref. 25) or IGRF with the standard Tsyganenko model (Ref. 26).

5. DISCUSSION: CURRENT MODELS, PREDICTION AND SPACE WEATHER IMPLICATIONS

For cosmic rays, CREME 96 (Ref. 27) is regarded as the most up-to-date and comprehensive model. It uses Nymmik's semi-empirical model for solar cycle modulation, which is based on the Wolf sunspot number and includes large scale structure of the heliospheric magnetic field. Agreement with observation is good with errors of the order of 25% on average as can be seen in Figure 14. This is to some extent surprising since we know that the modulation is not directly related to the sunspot number but is determined by equation (1) (section 2.2). Clearly the terms in equation (1) are all related to conditions on the sun and in the heliosphere and hence intimately connected to space weather. The question is whether or not an accuracy of 25% is acceptable. The answer to this and the question of prediction times of cosmic ray fluxes will to a great extent depend on the application or end-user. A full discussion of these issues cannot be given here but need to be addressed. CREME 96 also incorporates the multiply charged ACR component (above 20 MeV/nucleon) from SAMPEX results; because these ions are multiply charged, they will be geomagnetically shielded more effectively and so do not pose the same threat that they were once thought to (when considered to be only singly charged).

The JPL-91 model (Ref. 28) is the best and currently accepted model for solar proton events. It is however a statistical model that can predict fluences at energies >1, 4, 10, 30 and 60 MeV, with a given confidence level, for periods greater than 1 year. It should be continuously updated and needs to be extended to higher energies. It cannot predict when an event will occur, how big that event will be (e.g. > 10 MeV fluence) or what the spectral shape will be. Prediction of SPEs has not been addressed in the literature very much at all, no doubt due to the difficulty of the problem given that the events would appear to be random (Ref. 29). Details of the algorithms and techniques for the current prediction techniques used by the Space Environment Centre (SEC) are not easily obtainable. Three day forecasts are given with a probability of an event occurrence for each day. Another SEC algorithm, which was specifically developed for the Apollo lunar missions, is based on X-ray flares. An assessment of its performance for solar cycle 21 showed that less than 1% of events were missed but that 46% of the predictions were false alarms. As X-ray events are used, prediction times are only of the order of a few hours, although like the current methods, probabilistic forecasts of 1, 2 and 3 days ahead can also be generated. The strong association with CMEs and CME-driven shocks would suggest that prediction of these events would aid in the prediction of SPEs. But not all CMEs will produce SPEs at the earth; effective acceleration of protons will occur only if the CME is moving supersonically with respect to the local solar wind and the CME should also be moving towards the earth. Observation of the CME is not sufficient since when it has been observed the energetic particle will reach the earth in a matter of tens of minutes.

6. CONCLUSIONS

The paper has concentrated on the basic physical processes involved in the origin and acceleration, propagation and time dependencies of cosmic rays and solar protons and their interaction with earth's magnetic field (geomagnetic shielding). Where possible these processes have been illustrated with observational data. A brief description of current models has been given along with some comments on their accuracies and inadequacies. For cosmic rays, long term solar cycle modulations would appear to be well described by the CREME 96 model . However, the issue of what accuracy is actually needed by the user must be addressed as does that of prediction of short term variations (if it turns out that there is a requirement for these). The basic physics of solar-cycle modulation of cosmic rays appears to be well understood and there is a wealth of data available. The development of a more physically realistic model (i.e. not based on sunspots) would be possible and should lead to better accuracies than the CREME model but the issue is whether or not this is warranted from a user point of view.

For solar protons, the situation is not so clear in that we do not fully understand their causes. Nevertheless, the shift from a flare to a CME paradigm has done much to increase our understanding. Emphasis and future research for a predictive capability should be towards the development of a predictive capacity for not only the occurrence of CMEs but also their velocity and direction of travel. While progress in this area is likely to come from the solar physics community through more and better observations (e.g. SOHO) coupled with improved modelling (MHD, plasmas), other user-defined parameters such as prediction time and false alarm rate should be investigated since neural network techniques may provide a much faster (computationally) operational tool (but with less capability, i.e. probability of an event of unspecified size).

More data analysis and modelling of geomagnetic transmission is needed in order to be able to predict more accurately cut-off depression during geomagnetically active periods. The coincidence of large solar proton events, high geomagnetic activity and the formation of new trapped populations is not particularly well understood: do SPEs have a causal role in disturbing the magnetosphere and which SPEs will give rise to a new trapped population and under what conditions, for example. There is a need for a simple, but more accurate than Störmer theory, model for geomagnetic transmission factors during high geomagnetic activity which is not enormously computationally expensive (i.e. does not need supercomputer runs of days).

7. REFERENCES

1. Biermann, P, Origin of galactic cosmic rays 1995, *Phys. Rev. D,* 51, 3452-3454.
2. Mewaldt, R A, Cummings, A C, Adams, J H, Evenson, P, Fillius, W, Jokipii, J R, McKibben, R B & Robinson, P A, Toward A Descriptive Model of Galactic Cosmic Rays in the Heliosphere 1988, *Interplanetary Particle Environment,* Feynman, J & Gabriel, S B (editors), JPL Publication 88-28.
3. Evenson, P, Time Variation of Galactic Cosmic Rays, *ibid.,* p 149 – 161.
4. Global Processes That Determine Cosmic Ray Modulation 1998, Report of Working Group 1, Fisk, L A & Wenzel, K P (co-chairs), *Space Science Reviews 83*: 179-214.

5. Lockwood, J A & Webber, W R 1996, Comparison of the rigidity dependence of the 11-year cosmic ray variation at the earth in two solar cycles of opposite magnetic polarity, *J. Geophys. Res*., 101, 21573-21580.
6. Mewaldt, R A 1988, Elemental Composition and Energy Spectra of Galactic Cosmic Rays, *Interplanetary Particle Environment*, Feynman, J & Gabriel, S B (editors), JPL Publication 88-28.
7. Smart, D F & Shea, M A 1989, Solar Proton Events During the Past Three Cycles, *J. Spacecraft and Rockets*, 26, 403.
8. Feynman, J & Gabriel, S B 1996, High Energy Charged Particles in Space at One Astronomical Unit, IEEE Trans. *Nucl. Sci.* 43, 344.
9. Gosling, J T 1993, The Solar Flare Myth, *J. Geophys. Res*., 98, 18937.
10. Pudovkin, M I 1995, Comment on 'The solar flare myth' by J T Gosling, *J. Geophys. Res*., 100, 7917.
11. Reames, D V 1996, Energetic Particles from Solar Flares and Coronal Mass Ejections, in High Energy Solar Physics, Eds. R Ramaty, N Mandzhavidze, X-M Hua, *AIP Conf. Proc*. 374, p. 35.
12. Shea, M A 1988, Intensity/Time Profiles of Solar Particle Events at One Astronomical Unit, *Interplanetary Particle Environment*, Feynman, J & Gabriel, S B (editors), JPL Publication, 88-28.
13. Smart, D F & Shea, M A 1985, Galactic Cosmic Radiation and Solar Energetic Particles, in *Handbook of Geophysics and the Space Environment*, A S Jursa, Ed., Air Force Geophysics Laboratory, Bedford, MA, Ch. 6.
14. Barouch, E, Gros, M & Massa, P 1971, The Solar Longitudinal Dependence of Proton Event Decay, *Sol. Phys.*, 19, 483.
15. Smart, D F & Shea, M A 1996, The Heliolongitudinal Distribution of Solar Flares Associated with Solar Proton Events, *Adv. Space Res*., 17, 116.
16. Feynman, J, Armstrong, T P, Dao-Gibner, L & Silverman, S M 1990, A new interplanetary proton fluence model, *J. Spacecraft and Rockets*, 27, 403.
17. Feynman, J, Armstrong, T P, Dao-Gibner, L & Silverman, S M 1990, Solar Proton Events During Solar Cycles 19, 20, and 21, *Solar Physics*, 126, 385.
18. Störmer, C 1955, *The Polar Aurora*, Clarendon Press, Oxford.
19. Smart, D F & Shea 1994, M A, Geomagnetic Cutoffs : A Review for Space Dosimetry Applications, *Adv. Space Res*. 14, 796.
20. Klecker, B 1996, Energetic Particle Environment in Near-Earth Orbit, *Adv. Space Res*., 17, 45.
21. Lemaitre, G & Vallarta 1936, *Phys. Rev*., 50, 493.
22. Gussenhoven, M S, Mullen, E G & Brautigam, D H 1996, Improved Understanding of the Earth's Radiation Belts from the CRRES Satellite, IEEE Trans. *Nucl. Sci*. 43, 353.
23. Boberg, P R, Tylka, A J, Adams, J H, Flückiger, E O & Kobel, E 1995, Geomagnetic transmission of solar energetic protons during the geomagnetic disturbances of October 1989, *Geophys. Res. Lett*. 22, 1133.
24. Tsyganenko, N A 1989, A magnetospheric magnetic field model with a warped tail current sheet, Planet. *Space Sci*., 37, 5.
25. Nimmik, R A 1991, An approach to determination of real cosmic ray cut-off rigidities, *Proc. 22nd Internat. Cosmic Ray Conf.*, 3, 652.
26. Flückiger, E O, Kobel, E, Smart, D F & Shea, M A 1991, A new concept for the simulation and visualization of cosmic ray particle transport in the Earth's magnetosphere, *Proc. 22nd Internat. Cosmic Ray Conf., 3*, 648.
27. Tylka, A J, Adams, J H, Boberg, P R, Brownstein, B, Dietrich, W F, Flueckiger, E O, Petersen, E L, Shea, M A, Smart, D F & Smith, E C 1997, CRÈME 96: A Revision of the Cosmic Ray Effects on Micro-Electronics Code, IEEE Trans. *Nucl. Sci*., 44, 2150.
28. Feynman, J, Spitale, G, Wang, J & Gabriel, S 1993, Interplanetary Proton Fluence Model: JPL 1991, *J. Geophys. Res*., 98, 13281.
29. Gabriel, S B, Feynman, J & Spitale, G, Solar energetic particle events: statistical modelling and prediction**,** *ESA Symposium Proceedings on Environment Modelling for Space-based Applications*, p.59 (1996).

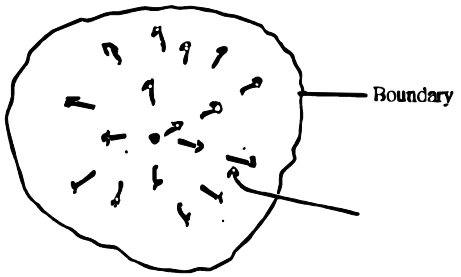

Balance between (1) **T)iftsion**
(2) Convection
(3) Deceleration

Fig. I Schematic representation of solar modulation (From Ref. 3)

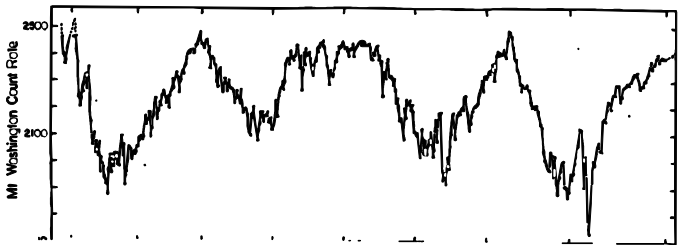

Fig. 2 The 26-day average Mount Washington neutron monitor count ratefrom 1955 to 1995. The datafor 1955 have not been normaided, and the preliminary data in late 1995 are indicated by the dashed line (From Ref. 5)

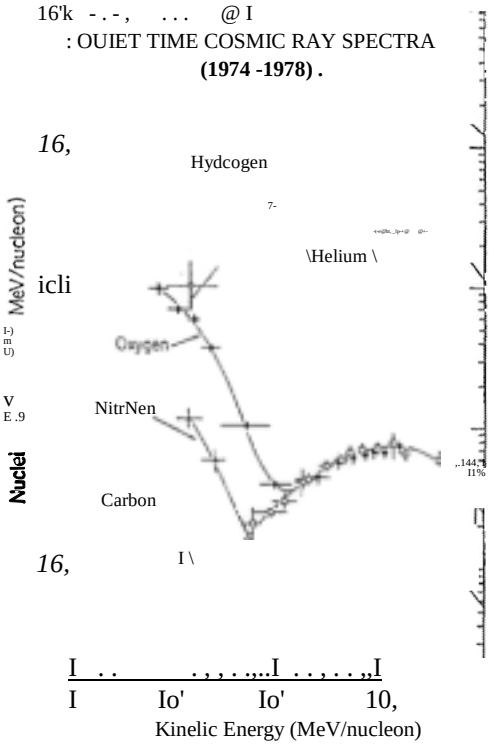

Fig. 3 Typical cosmic ray spectra (From Ref 6)

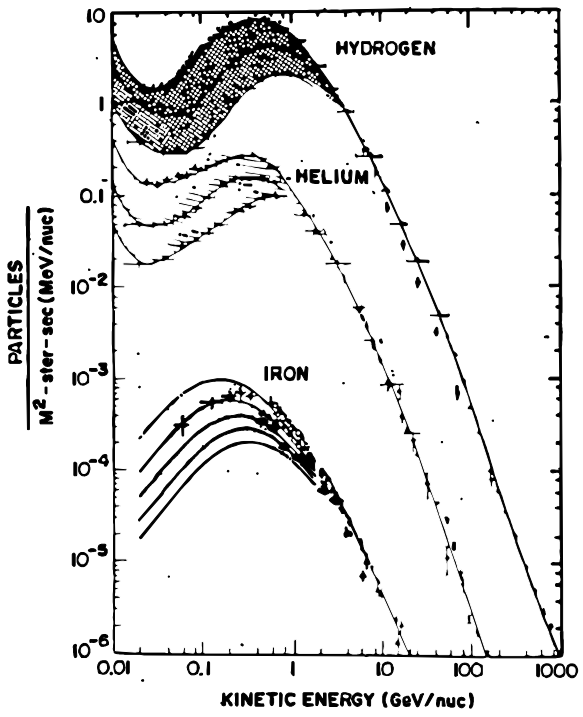

Fig. 4 Cosmic ray energy spectra showing magnitude of solar modulation (From Ref 7)

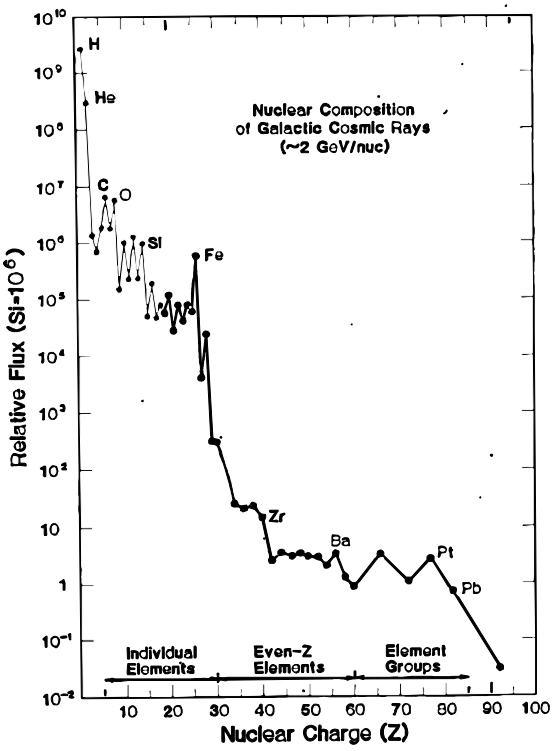

Fig. 5 The relativeflux of cosmic rays as afunction of nuclear charge Z (From Ref 6)

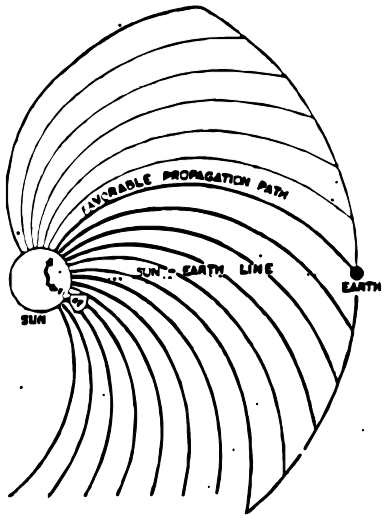

Fig. 6 Propagation ofsolar energetic particles. Those propagating along the 'Yavorable path" will be anisotropic at Earth (From Ref 12)

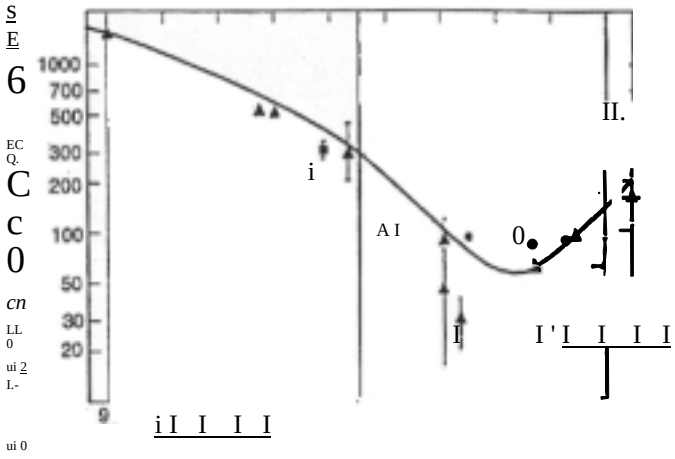

Fig. 7 Longitudinal distribution ofpropagation times of solar particiesftom their source to the Earth. The various symbols indicate datafrom dif .ferent studies. The line is added to guide the eye From Refs. 13 and 14)

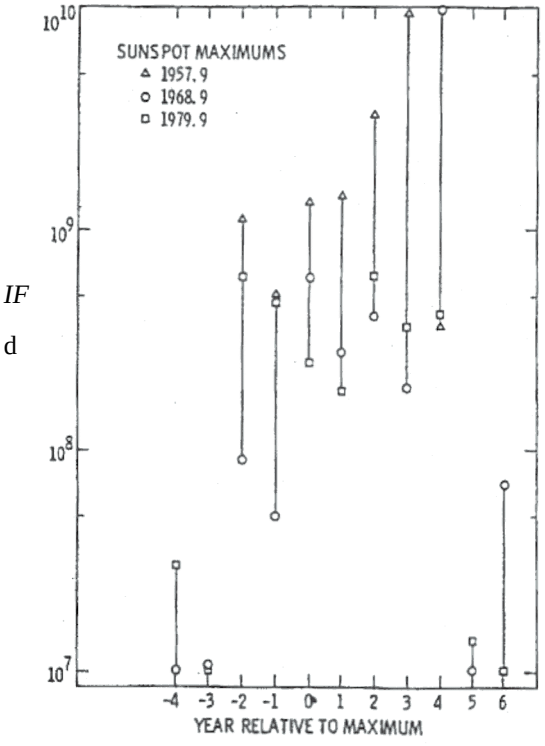

Fig. 8 Solar cycle variation ofyearly integratedj7uences (E > 30 Me @9 observed at 1.4 U (From Ref 14)

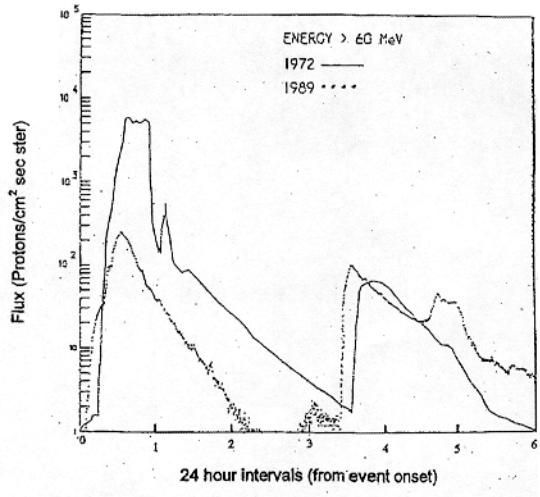

Fig. 9 Proton fluxes for two major solar proton events (E > 60 MeV). Data from IMP 8 (From Ref. 8)

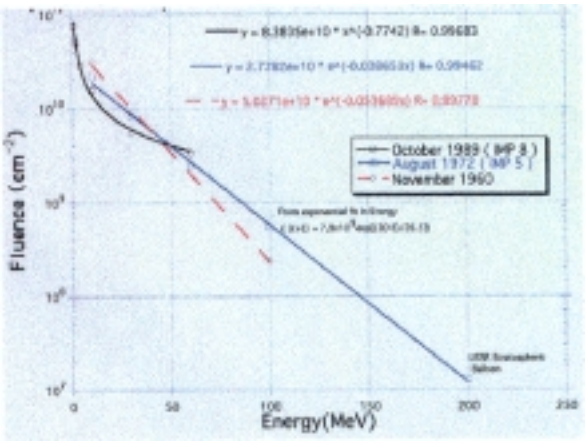

Fig. IO Fluence spectra of 3 large solar proton events

5@9@g9tg9u

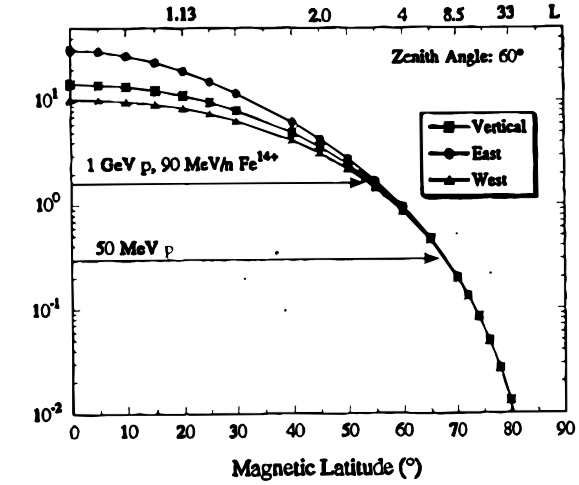

Fig. 11 Cutoff rigidity in the dipole approximation of the Earth's magneticfzeldfor west, east and vertical Directions as a function of magnetic latitude (From Ref. 20)

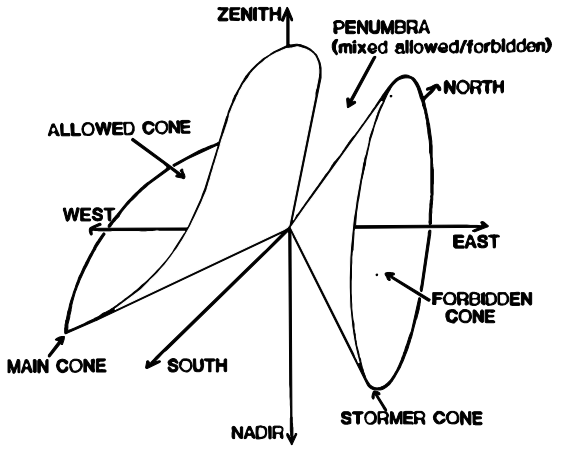

Fig. 12 Geometric visualization of cutoffs (From Ref. 17@

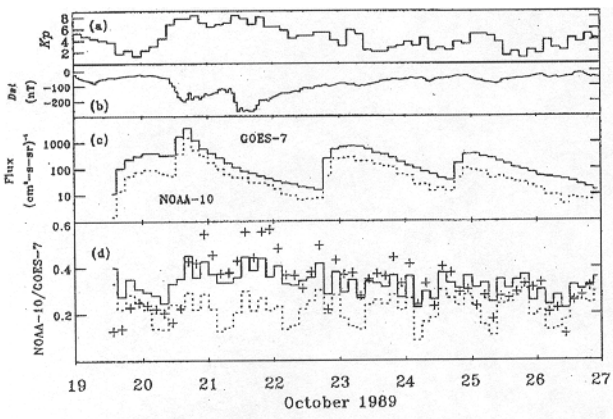

Fig. 13 Geomagnetic transmission during high geomagnetic activity : observations and modelling. Crosses indicate 3-hour averaged NOAA-10/GOES 7, solid line IGRF + modified Tsyganenko 89 and dashed line IGRF grid (From Ref. 23)

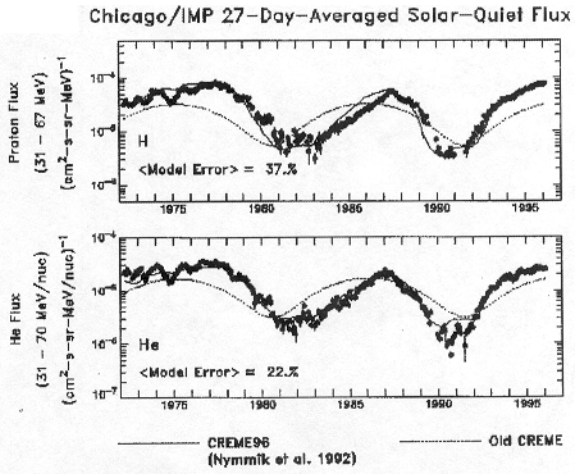

Fig. 14 Cosmic ray model : solar cycle modulation, CREME 96 compared to Chicago IMP 8/CRT data (From Ref. 27)